Bull. Chem. Soc. Ethiop. **2020**, 34(1), 105-121. ISSN 1011-3924
© 2020 Chemical Society of Ethiopia and The Authors Printed in Ethiopia
DOI: https://dx.doi.org/10.4314/bcse.v34i1.10

PREPARATION AND SORPTION PROPERTY STUDY OF $Fe_3O_4/Al_2O_3/ZrO_2$ COMPOSITE FOR THE REMOVAL OF CADMIUM, LEAD AND CHROMIUM IONS FROM AQUEOUS SOLUTIONS

Fekadu Tsegaye[1], Abi M. Taddesse[2*], Endale Teju[2] and Minbale Aschalew[2]

[1]Haramaya University, Central Laboratory, P.O. Box 138, Dire Dawa, Ethiopia
[2]Haramaya University, College of Natural and Computational Sciences, Department of Chemistry, P.O. Box 138 Dire Dawa, Ethiopia

(Received May 17, 2018; Revised October 11, 2019; Accepted October 21, 2019)

ABSTRACT. Fe-Al-Zr ternary mixed oxides composite was synthesized via co-precipitation method for the removal Pb(II), Cd(II) and Cr(VI) ions from aqueous solutions. The as-synthesized materials were characterized by X-ray diffraction (XRD), Brunauer-Emmett-Teller (BET), scanning electron microscope hyphenated with energy dispersive X-ray diffraction (SEM-EDX) and Fourier transform infrared (FTIR) techniques. The pH at the point of zero charge (pH_{pzc}) of the sorbent and effect of ionic strength on sorption were also determined. The batch tests were conducted to optimize the various sorption parameters such as pH, adsorbent dose, contact time, speed of agitation and initial metal concentration. The experimental results showed that the adsorbed amounts of Pb(II), Cd(II) and Cr(VI) tend to decrease with increase in pH. Freundlich isotherm model fits better the equilibrium data for the adsorbent. Kinetic data correlated better with both pseudo first order and pseudo second order kinetic models. The spontaneous nature of the adsorption process was also confirmed from thermodynamic grounds. The nanosized adsorbent exhibited an adsorption efficiency of 96.65%, 96.55% and 97.2% for Cd(II), Cr(VI) and Pb(II), respectively, at optimum condition. Experimental results showed that the nanocomposite was effective for the removal of the title heavy metals from aqueous solution.

KEY WORDS: Adsorption, Nanocomposite, Heavy metal, Wastewater, Ternary oxides

INTRODUCTION

Heavy metals pollution to the environment is a consequence of several activities like chemical manufacturing, painting and coating, tanning, mining, extractive metallurgy, nuclear and other industries [1]. These metals exert a deleterious effect on fauna and flora of lakes and streams [2]. Most of the heavy metals are toxic and due to their non-biodegradability and persistence, they tend to accumulate in living organisms causing various diseases and disorders. Nickel, cadmium, mercury, zinc, lead and chromium are examples of toxic heavy metals that are produced by industries which pose a risk of contaminating groundwater and other water resources [3].

Various treatment techniques are practiced for removal of toxic heavy metals from water and wastewaters. These methods are biological methods, ion exchange [4], combined chemical and biochemical methods [5], chemical oxidation and photo-catalysis [6-8], adsorption [9], coagulation and membrane treatments [10]; each of these has its own specific advantages and disadvantages. Adsorption could be a very good alternative technology for removal of heavy metal, especially at low concentration. The efficiency of adsorption depends on the adsorbent high surface area to volume ratio, morphology, pore size distribution, polarity, and functional groups attached to the adsorbent surface [11]. The principal types of adsorbents include activated carbon [12], synthetic polymers [13] and silica-based adsorbents [14]. However, these adsorbents are not often used for wastewater adsorption because of their high cost. Hence, there

*Corresponding author. E-mail: abi92003@yahoo.com

is a recent need for the development of a method that is highly selective, more efficient, easy to operate and hence cost effective.

Nanocomposite adsorbents are one class of nanomaterials synthesized for applications in sorption processes to remove ions and various contaminants from environment and water. Transition metal oxides are one of the most important compounds for synthesis of nanocomposite sorbents. For example iron oxides are used to synthesize nanocomposite adsorbent either in pure form or with other transition metal oxides [15]. Although iron oxides alone have several applications, some of their adsorptive properties can be improved when prepared in mixture with other metal oxides such as Al(III), Cr(III), Cu(II), Mn(IV), Ti(IV) and Zr(IV) [16]. Recently, the development of nanoscience and nanotechnology has shown remarkable potential for the remediation of environmental problems [17]. Compared with traditional materials, nanostructure adsorbents have exhibited much higher efficiency and faster rates in water treatment.

Several heavy metals removing adsorbents have been proposed including nanosized ferric oxides, zirconium oxides, aluminum oxides and application of mixed ferrous/ferric iron hydroxides. Many researchers reported the effective use of nanocomposite such as Glauconite, Amino-modified Fe_3O_4 MNPs [18], m-PAA-Na-coated MNPs [19] and Fe_3O_4-GS [20] on heavy metal removal from wastewater. The magnetic nanoparticle (MNP) adsorption has attracted much interest and is an effective and widely used process because of its simplicity and easy operation [21]. The magnetic nanoparticles exhibit amphoteric surface activity, easy dispersion ability and, to their very small dimensions, a high surface-to-volume ratio, resulting in a high metal adsorption capacity [22], small size and magnetic property.

To the best of the researchers' knowledge, little work has been done using ternary composite as adsorbents to remove toxic heavy metals from aqueous solutions. Hence, the main objective of this paper was to evaluate cadmium, chromium and lead removal efficiency of $Fe_3O_4/Al_2O_3/ZrO_2$ composite sorbent from aqueous solution.

EXPERIMNTAL

Synthesis of the adsorbent

The ternary oxide nanocomposite adsorbent with percentage composition Fe:Al:Zr 70:25:5 was prepared by chemical co-precipitation method as reported by [23]. In the first step, stochiometric amount of the precursors for magnetite namely, $FeCl_2{\cdot}4H_2O$ and $FeCl_3.6H_2O$ were accurately weighed and the calculated amounts were dissolved in 100 mL of 0.3 M HCl solution. Then, the solution was added drop wise from separatory funnel into the solution of 120 mL of 3 M NaOH over a period of 2 h, under vigorous stirring at 80 ^oC in N_2 atmosphere. During this process, the pH of mixture was kept at 12.0 using 0.1, 0.01 and 0.001 M NaOH or HNO_3 solutions. The suspension was left undisturbed for 4 h and then the settled phase was separated from the liquor and washed with deionized water several times to obtain a suspension of Fe_3O_4 ferrofluid. The magnetite–alumina–zirconia oxide nanocomposite was prepared by adding 100 mL of $Al(NO_3)_3.9H_2O$ and $ZrOCl_2.8H_2O$ (obtained by dissolving stoichiometric amounts of both salt in 100 mL of deionized water) into the obtained Fe_3O_4 suspension and ultrasonicated for 10 min prior to use. The pH of the mixtures was adjusted to 8.0 using 0.1, 0.01 and 0.001 M NaOH and HCl. Then mixture was magnetically stirred under N_2 atmosphere for 1.5 h at 70 ^oC. Finally the resulting magnetic compound was separated by permanent magnet, washed with deionized water several times to remove impurities such as Cl^-, NO_3^- and excess OH^- ions and then dried at 60 ^oC for 24 h to obtain the desired product.

Characterization of the nanosorbent

The structure of the as-synthesized sorbent was examined by powder X-ray diffraction (XRD) using X'Pert Pro PANalytical equipped with an X-ray source of a CuKα radiation (wavelength of 0.15406 nm) at step scan rate of 0.02 (step time: 1 s; 2θ range: 5.0–90.4). The morphology and particle size distribution of the solids were determined by scanning electron microscopy (SEM) using a Hitachi TM1000 with EDX detector. Specific surface areas were estimated by the Brunauer, Emmett and Teller (BET) method. The FTIR spectrum of the as-synthesized nanosorbent was determined using the KBr disc method. The IR absorption pattern was recorded between 400 and 4000 cm^{-1} using Shimadzu (1730, Japan) spectrometer. The percentages of iron as iron oxide in all the as-synthesized powder was determined using standard procedure by flame atomic absorption spectrophotometer.

Batch adsorption studies

Batch mode adsorption studies for Cr(VI), Pb(II) and Cd(II) were carried out in 50 mL Erlenmeyer flask. The batch adsorption process was optimized with respect to pH, adsorbent dose, speed of agitation, contact time and initial concentration. For each run, the resulting suspension of each ion was filtered using Whatman No. 41 filter paper and the filtrate was analyzed by FAAS. Removal efficiency of the adsorbent was finally determined by using the relationship given below.

$$\text{Adsorption } \% = \frac{(C_i - C_e)}{C_i} \text{ x } 100 \quad (1)$$

where C_i = the initial concentrations (mg/L) and C_e = final concentrations (mg/L) of the Cr (VI)/Pb (II)/Cd (II) ions. The adsorption capacity of Cr(VI)/Pb(II)/Cd(II) ions were the concentration of the Cr(VI)/Pb(II)/Cd(II) ion on the adsorbent mass and were calculated based on the mass balance principle,

$$Q_e = \frac{(C_i - C_e)V}{m} \quad (2)$$

where Q_e = adsorption capacity of adsorbent (mg/g), V = the volume of reaction mixture (L), m = the mass of adsorbent used (g), C_i = the initial concentrations (mg/L) and C_e= final concentrations (mg/L) of the Cr(VI)/Pb(II)/Cd(II) ion [3].

Optimization of parameters

In this work the effect of various adsorption parameters such as adsorbent dose, time, agitation speed, initial concentration, pH_{pzc}, and ionic strength have been determined.

Effect of solution pH

To study the influence of pH on the present adsorption process, experiments were carried out by adding 0.1 g of the adsorbent into 50 mL Erlenmeyer flask containing 25 mL of 30 mg/L of the respective metal ions. Then the pH of the solutions was varied to 2, 3, 4, 7 and 9 before adsorption experiments were carried out while keeping other parameters constant (agitation speed at 120 rpm and contact time at 24 h). Each time the pH of the solutions was adjusted with dilute HCl and/or NaOH solutions. Then equilibrium Cr(VI), Pb(II) and Cd(II)) ions concentrations were measured after the solutions were filtered. Then the pH at which maximum adsorption was obtained was taken as the optimum value for subsequent experiments [24].

Point of zero charge determination

The determination of point of zero charge (pzc) of the synthesized Fe-Al-Zr adsorbent was assessed. To this effect 50 mL of 0.001 M $NaNO_3$ solution was added to 0.1 g of Fe-Al-Zr ternary mixed oxide nanocomposite and adjusted to various pH values ranging from 2-12 by using dilute HNO_3 or NaOH solutions in a 250 mL beaker. After equilibrating the mixed solution for 60 min in a mechanical shaker the initial pH was determined. Then 1 g of $NaNO_3$ was added to the above and further equilibrated for another 60 min and the final pH was measured. The graph of $pH_{final\text{-}initial}$ (y-axis) versus pH_{final} (x-axis) was plotted from which the point of zero charge was determined as the point where the graph intersects the x-axis [28].

Effect of ionic strength

The effect of ionic strength (0.02 to 0.1 M $NaNO_3$) on the adsorption capacity of Fe-Al-Zr in the removal of Cd(II), Cr(VI) and Pb(II) was investigated. About 1 g, 0.1 g and 0.5 g of Fe-Al-Zr were placed in a 125 mL Erlenmeyer flask at an initial concentration of 20 mg L^{-1} and initial pH of 6, 4 and 6. The samples were agitated using a shaker bath at 120 rpm and 100 rpm for 12 h and 6 h, respectively [32].

Adsorption isotherms

The adsorption isotherms were used to characterize the interaction of each analyte ions with adsorbent. Equilibrium data are usually described by various adsorption isotherms. Two isotherm equations were used in the present study, Langmuir and Freundlich [28]. The Langmuir isotherm model assumes a monolayer adsorption of solutes onto a surface comprised of a finite number of identical sites with homogeneous adsorption energy, meaning once a lead molecule occupies a binding site, no further adsorption can happen at that site. The Freundlich isotherm model is valid for multilayer adsorption on a heterogeneous adsorbent surface with no uniform distribution of heat of adsorption [29]. The Langmuir equation is:

$$C_e/q_e = 1/(b\, q_{max}) + (C_e / q_{max}) \quad (3)$$

The Freundlich equation is:

$$\text{Log } q_e = \text{Log } K_f + (1/n)\, \text{Log } C_e \quad (4)$$

where q_e is the amount of adsorbed material at equilibrium (mg/g), C_e is the equilibrium metal ions concentration of the adsorbate (mg/L), q_{max} (mg/g) and b (L/mg) are the Langmuir constants, and K_f and n are Freundlich constants.

Adsorption kinetics

The adsorption kinetics of Pb(II), Cr(VI) and Cd(II) ions were determined by varying the contact time as, 3, 6, 12, 16, 24 and 48 h by keeping all parameters (pH, adsorbent dose, contact time, agitation speed and initial concentration) at optimized values. For all the above parameters, percent of adsorption (%) was calculated using the following equation [25].

$$\text{Percent of adsorption (\%)} = \frac{C_o - C_e}{C_o} \times 100 \quad (5)$$

where C_o and C_e are the initial and final (equilibrium) concentrations of metal ion in solution (mg/L).

Thermodynamic study

In order to determine the effect of temperature on sorption phenomenon, all predetermined and optimized values of the parameters were used and the temperature was established at 30, 40, 50 and 60 ^oC. The thermodynamic parameters such as change in standard free energy (ΔG), enthalpy (ΔH) and entropy (ΔS) can be calculated by using the following equation [30].

$$\Delta G = -nRTlnK_c \quad (6)$$

$$\Delta G = \Delta H – T\Delta S \quad (7)$$

$$lnK_c = \Delta S/R - \Delta H/RT, \text{ where } lnK_c = q_e/C_e \quad (8)$$

where R (8.314 J/molK) is the gas constant, T (K) is the absolute temperature and K_c (cm^3g^{-1}) is the standard thermodynamic equilibrium constant defined by q_e/C_e.

Desorption study

The powder was immersed in the regenerating solution and placed in a shaker at 25 ^oC for 12 h. To this, 0.1 M NaOH solution was added for desorption to take effect. The desorbed adsorbate in the solution was finally recovered by filtration and analyzed for the corresponding metal ion concentration. The recovery percentage was obtained from the following relation:

$$\text{Desorption efficiency } \% = \frac{\text{Desorbed}}{\text{Adsorbed}} \times 100 \quad (9)$$

where, desorbed = the concentration and/or the mass of the metal ion after the desorption process. Adsorbed = $(C_o – C_e)$ for each recovery process.

Recyclability study

To investigate the extent of regeneration and reusability of the adsorbent, metal ion solutions of constant feed concentration (20 mg/L) was run through the optimum dose (0.1, 0.5 and 1 mg) of the adsorbent for 6 and 4 h. After the completion of each run, the adsorbent were washed thoroughly with 0.1 M NaOH solutions, for 15 min in continuous recycle modes. Desorption of metal ion by 0.1 M NaOH solution was reported. Next, the systems were washed with distilled water for 3 min, until the permeate would have the same pH as cleaning water. After washing, permeability value was checked [31].

RESULTS AND DISCUSSION

Characterization of as-synthesized adsorbent

X-ray diffraction (XRD) is one of the most important non-destructive tools to analyze all kinds of matter-ranging from fluids, to powders and crystals. From research to production and engineering, it is an indispensable method for materials characterization and quality control [33]. The XRD patterns of Fe-Al-Zr ternary oxide nanocomposite before (upper) and after (lower) adsorption experiments were demonstrated in Figure 1. The broad background suggests the amorphous nature of the composite. However, the presence of very weak intensity peaks at 2θ values 35.25, 43.32, 43.42, 53.69 and 63.33° showed the formation of some crystal at very small scale up on formation of nanocomposite structure [34]. These 2θ values could be assigned to a face centered cubic spinel structure of magnetite (Fe_3O_4). This result agrees with previous reports made by [23]. The relatively similar peak intensities before and after sorption indicates the potential for repeated usage of the sorbet. No peak attributable to alumina and zirconia was observed in this composite. This could due to absence of calcinations making the material

predominantly amorphous. For example, crystallized alumina such as γ-Al_2O_3 and α-Al_2O_3 could be expected under thermal treatment with temperature at 800 ^oC and 1000 ^oC respectively [30], where as monoclinic or tetragonal phases are expected in the temperature range from 600– 800 ^oC [45].

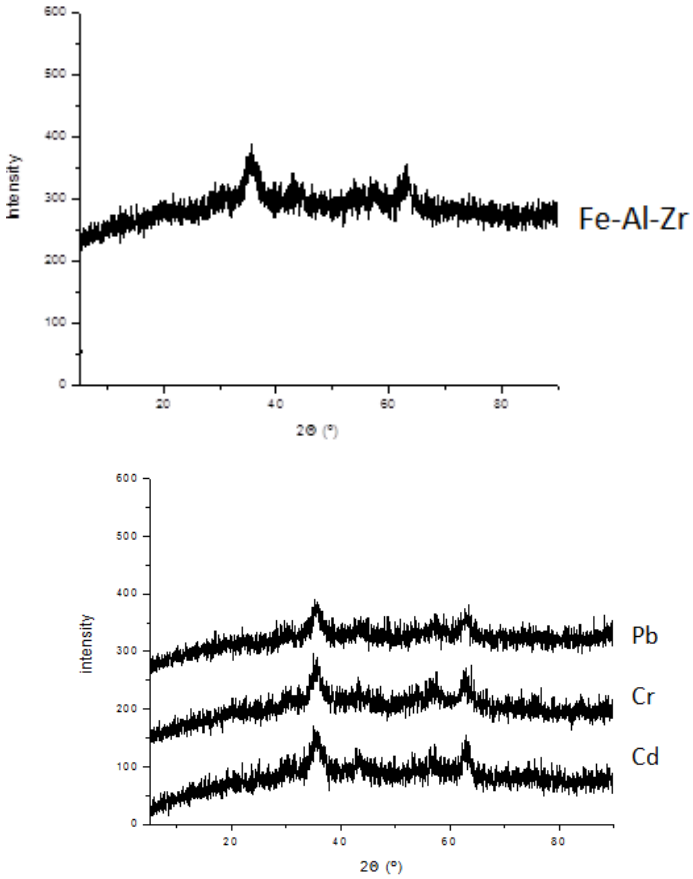

Figure 1. XRD pattern of Fe-Al-Zr before adsorption (upper) and XRD pattern of Fe-Al-Zr after adsorption of Pb (II), Cr (VI) and Cd (II) (lower).

The FT-IR spectra of ternary nanocomposite display a number of peaks before and after adsorption (Figure 2). The peaks observed in all cases were more or less similar. The absorption bands observed from (3500–3000 cm^{-1}) centered at 3424, 3414 and 3412 cm^{-1} represent O-H stretching vibrations of adsorbed water molecules. The peaks at 2923 and 2853 cm^{-1} represent anti-symmetrical and symmetrical H–O–H stretching vibrational modes [46]. The absorption bands observed at 1626-1628 and 1375 cm^{-1}could be attributed to H-O-H bending vibration and Al-O stretching respectively and the strong Fe–O absorption bands around 583.5-591.48 cm^{-1} corroborates that the main phase of as-prepared particles is magnetite. Another important adsorption band can be observed at 441.45 cm^{-1}, which corresponds to the vibration of the Zr-O bond in the Fe-Al-Zr powders [36].

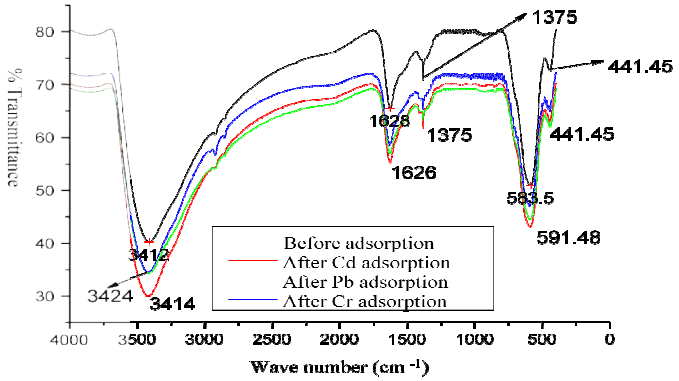

Figure 2. FT-IR spectra of $Fe_3O_4/Al_2O_3/ZrO_2$ before (black) and after (colored), respectively.

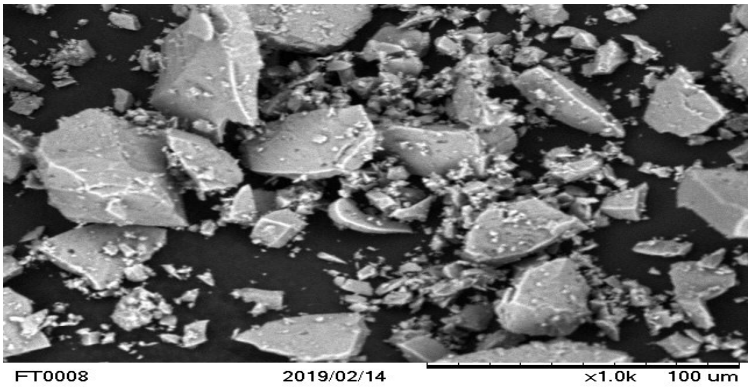

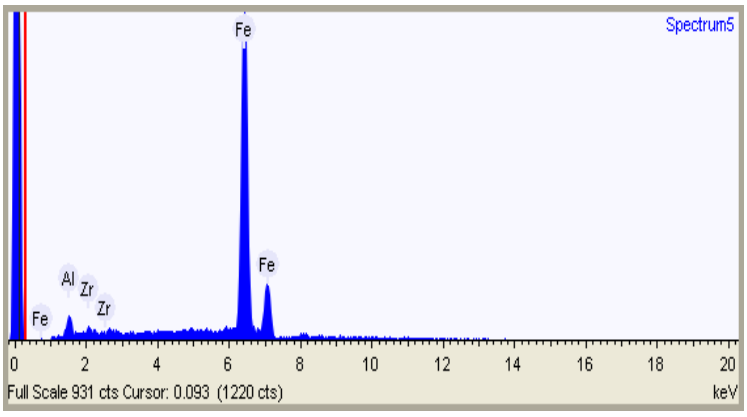

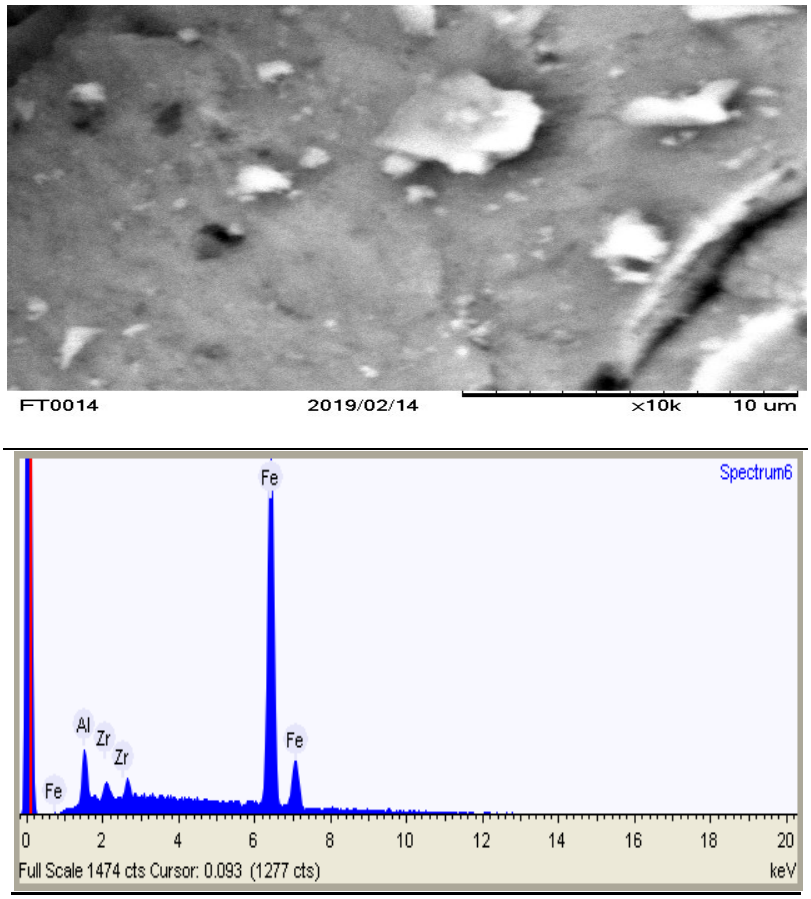

Figure 3. SEM- EDX micrographs of Fe-Al-Zr composite.

The SEM image of the ternary composite showed plate like structures with less consistency (Figure 3). A closer look of the image (FT008) displayed at (FT0014) revealed presence of porous structures, and brighter deposits on the surface of the host magnetite possibly indicated the presence of ZrO_2. The EDX spectra exhibited the presence of Fe, Al and Zr components. The percentage compositions of Fe, Al and Zr from all the EDX spectra (data not shown) in the as synthesized sorbent was found to be 72.3, 23.9 and 3.8%, respectively, not far from the expected values of the oxides; 70% for iron, 25% for aluminum and 5% for zirconium. The difference between the experimental and expected values could be due to insufficient dissolution, vaporization and lack of atomization.

The specific surface area of the Fe-Al-Zr based sorbent was found to be 205 m^2g^{-1} indicating the moderately large specific surface area of the as-synthesized powder compared with similar ternary oxide systems such as Mn-Al-Fe (41 m^2g^{-1}), Cu-Fe-Al (82.61 m^2g^{-1}) and Ni-Al-Fe (111 m^2g^{-1}) [35, 42]. Nonthless, higher BET results have also been reported for the ternary systems such as Fe-Al-Mn (303 m^2g^{-1}) [43], and Y-Zr-Al trimetalic oxides (256.6 m^2g^{-1}) [44].

Optimum conditions

Batch mode of adsorption was conducted to optimize parameters such as adsorbent dose, speed of agitation, contact time and initial metal concentration. The respective optimum values were found to be pH 6, 6 and 4; adsorbent dose 0.5, 1 and 0.1 g; agitation speed 100, 100 and 120 rpm; contact time 6,6 and 12 h and initial metal concentration of 20 mg/L for Pb(II), Cd(II) and Cr(VI), respectively.

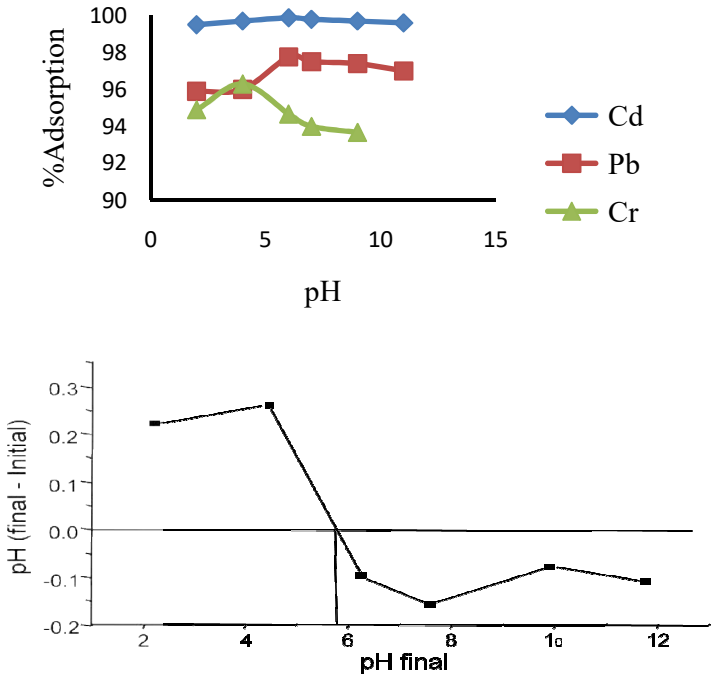

Figure 4. Effect of pH on the removal Pb, Cd and Cr at initial concentration ions (Co = 30 mg/L dose = 0.1 g, agitation speed = 120 rpm and contact time = 24 h) (upper) and pH point zero charge (pH_{pzc}) for $Fe_3O_4/Al_2O_3/ ZrO_2$ (lower).

The as-synthesized Fe-Al-Zr sorbent displayed a maximum Pb(II), Cd(II) and Cr(VI) removal efficiencies of 97.8%, 99.8% and 96.3% at the optimized pH values. The effect of pH on the extent of adsorption of Pb(II), Cd(II) and Cr(VI) ions onto the nanocomposite adsorbent was investigated by varying the pH from 2 to 9 keeping other parameters constant. Maximum sorption was registered for Cd(II) and Pb(II) ions at pH 6. At this pH, the surface of the sorbent is anticipated to be negative given the 5.71 pH_{pzc} (Figure 4) making the sorbent amenable for cation sorption mainly as the result of electrostatic attraction. Beyond this optimum pH, the sorption of the cations drops due to electrostatic repulsion between the cations and hydronium ions at lower pH or due to precipitation when the pH is higher. Unlike Cd and Pb cations, Cr(VI) is an anion. That is why its sorption is greatest at pH 4. At this pH, the surface exhibits positive charge having greater affinity for anions. The sorption of Cr(VI) is found to be lower at extreme cases possibly due to repulsion at alkaline condition and dissolution of the sorbent at strongly acidic condition.

Adsorption isotherm

The Langmuir isotherm model describes the adsorption of an adsorbent on a homogeneous, smooth surface of an adsorbent, and each adsorptive site can be occupied only once [29]. The empirical Freundlich model is based on the sorption on reversible heterogeneous surfaces [37]. Langmuir and Freundlich adsorption constants and coefficients of determination (R^2) are presented in Table 1. To find the most appropriate model for the metal ions adsorption; data were fitted to Freundlich isotherm models. Results revealed that Freundlich adsorption isotherm was the best model for the metal ions adsorption onto Fe-Al-Zr with R^2 of 0.9846, 0.9737 and 0.9239 for Cd(II), Cr(VI) and Pb(II), respectively.

Table 1. Langmuir and Freundlich isotherm constants for Cd(II), Cr(VI) and Pb(II) ions adsorption by Fe-Al-Zr ternary mixed oxide.

Ion	Langmuir isotherm model				Freundlich isotherm model		
Parameter	Q_{max}	b	R_L	R^2	K_f	n	R^2
Cd	4.38	0.11	0.3	0.8760	0.54	1.74	0.9846
Cr	26.8	0.21	0.19	0.8865	4.77	1.80	0.9737
Pb	9.44	0.036	0.58	0.8057	0.56	1.67	0.9239

Kinetics of adsorption

The kinetics of Cd(II), Cr(VI) and Pb(II) adsorption on the Fe-Al-Zr ternary composite were analyzed using pseudo first-order and pseudo second-order kinetics models (Figure 5). The conformity between experimental data and the model predicted values was expressed by the coefficient of determination (R^2). As seen in Table 2, the value of R^2 calculated from pseudo-second order kinetics was a little higher than pseudo first order; however, it appeared that both The values of rate constant (k) and coefficient determination (R^2) are as reported in Table 2 for the two models.

Table 2. The values of parameters and correlation coefficients of kinetic models.

	Cd			Cr			Pb		
	k	q_e (mg/g)	R^2	k	q_e (mg/g)	R^2	k	q_e (mg/g)	R^2
Pseudo first order	0.065	0.043	0.9946	0.079	0.0575	0.9956	0.075	0.04	0.9995
Pseudo second order	1.73	0.646	0.9958	1.37	6.57	0.9967	3.7	1.3	0.9998

Thermodynamics of adsorption

The thermodynamic parameters such as change in standard free energy (ΔG), enthalpy (ΔH) and entropy (ΔS) can be calculated by using the following equation:

$$\Delta G = -RT \ln Kc \quad (10)$$

$$\ln K_c = \frac{\Delta S}{R} - \frac{\Delta H}{RT} \quad (11)$$

where R (8.314J/mol K) is the gas constant, T(K) is the absolute temperature and K_c is the standard thermodynamic equilibrium constant defined by q_e/C_e. By plotting the graph of $\ln K_c$ versus T^{-1}, the value of ΔH and ΔS can be estimated from the slopes and intercept. The result of ΔG^0, ΔH^0 and ΔS^0 are shown in Figure 6. All the thermodynamic parameters are listed in Table 3. The negative values of Gibbs free energy for all the metal ions demonstrated that the

adsorption process was spontaneous. Furthermore, it was also verified by the fact that the enthalpy values of the adsorption (ΔH^0) were positive, characterizing the process as endothermic [6]. Additionally the positive entropy (ΔS^0) observed for all the metal ions indicated the increased randomness at the solid–liquid interface during the adsorption of Cd(II), Cr(VI) and Pb(II) [38] and the affinity of the adsorbents for Cd(II), Cr(VI) and Pb(II) ions [39].

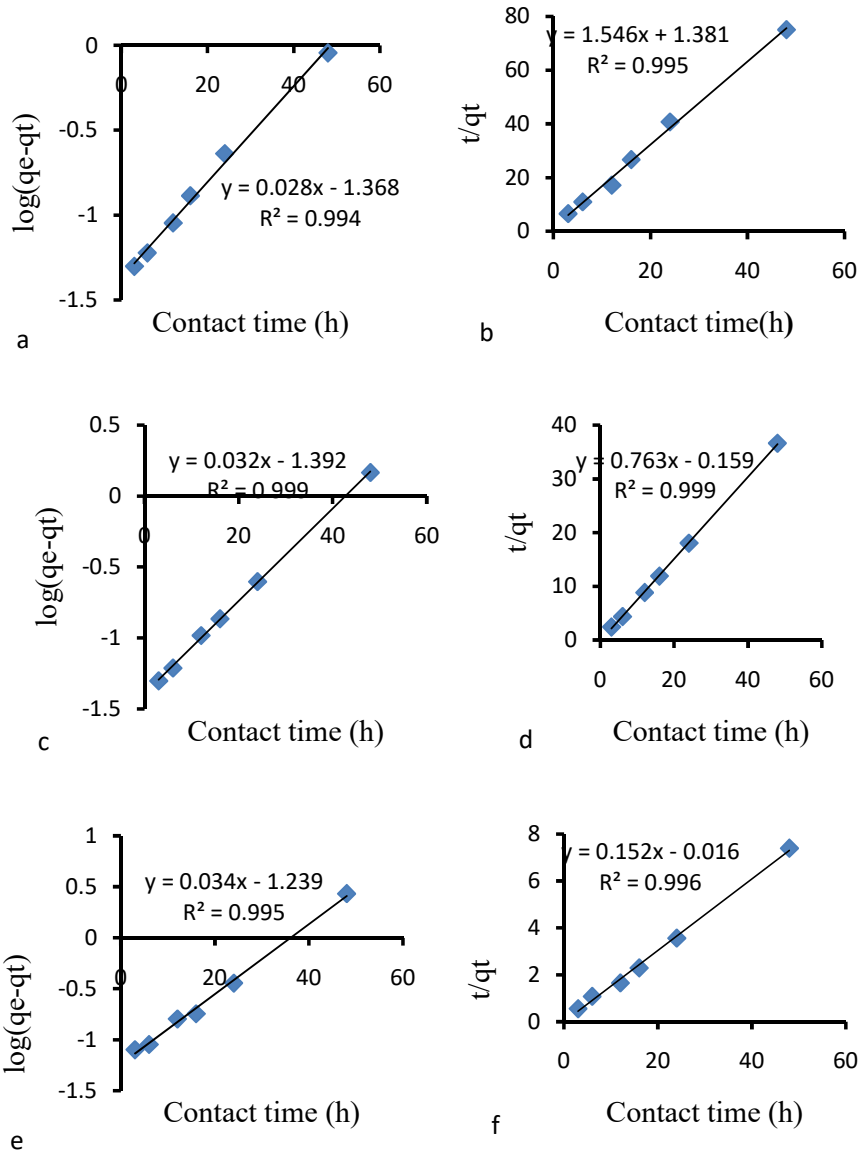

Figure 5. Plot of the pseudo-first order (a, c, and e) and pseudo-second order (b, d and f) onto Fe-Al-Zr nano sorbent, respectively.

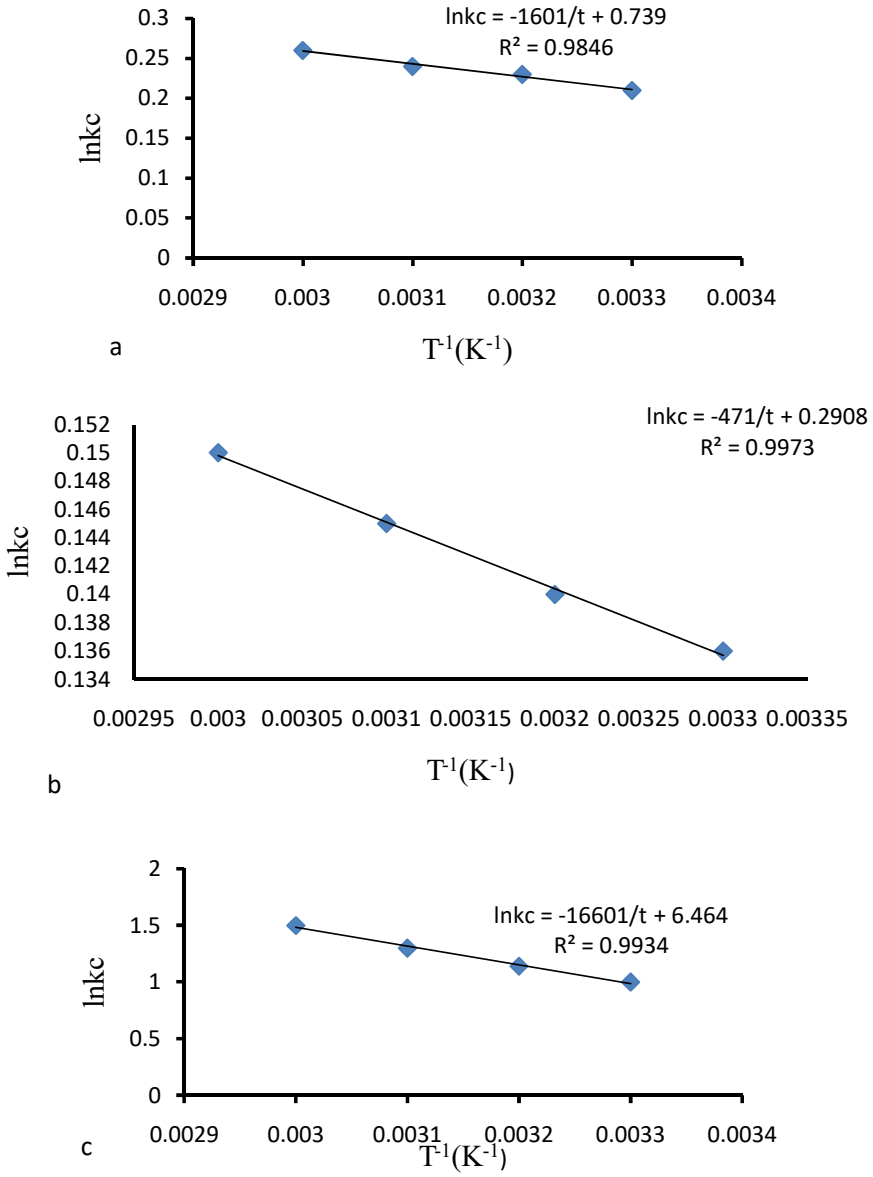

Figure 6. Plot of $\ln K_c$ vs T^{-1} for Pb(II), Cd(II) and Cr(VI) ions adsorption in Fe-Al-Zr sorbents.

Table 3. Thermodynamic parameters for Pb(II), Cd(II) and Cr(VI) ions adsorption onto $Al_2O_3/Fe_3O_4/ZrO_2$ adsorbent.

Ion	Temp. (K)	ΔG (kJ/mol)	ΔH (kJ/mol)	ΔS (J/molK)
Cd	303	-129.5	+365.8	+2.3
	313	-132.3		
	323	-135.1		
	333	-137.9		
Cr	303	-3445	+13053	+51.45
	313	-3507		
	323	-3569		
	333	-3631		
Pb	303	-383.9	+1330	+6.144
	313	-391.3		
	323	-398.7		
	333	-406.1		

Effect of ionic strength

Ionic strength is an important parameter especially when solute removal is affected by slight changes in the supporting electrolyte solution. The concentration of $NaNO_3$ was varied from 0.0 to 0.1 M, where % removal of sorbent in removing Cd(II), Cr(VI) and Pb(II) were calculated. The results showed the % removal of the heavy metals in the absence of $NaNO_3$, removal Cd(II), Cr(VI) and Pb(II) were 99.8, 93 and 94%, respectively and in the presence of 0.1 M $NaNO_3$, the % removal were observed to decrease to 96, 87 and 82% for Cd(II), Cr(VI) and Pb(II), respectively. As the concentration of $NaNO_3$ increases, the % removal was decreased due to the accumulation of charge in the vicinity of the Fe-Al-Zr surfaces. Upon addition of $NaNO_3$, the cation Na^+ would be distributed in the outer layer surrounding the Fe-Al-Zr ternary nanocomposite sorbent. The removal of Cr(VI) decreased by 6% on the basis of stated ionic strength. This is presumed to be due to competition of NO_3^- with $HCrO_4^-$ or CrO_4^{2-} with the surface of Fe-Al-Zr, and with increasing ionic strengths 0-0.1 mol L^{-1}, the electrostatic repulsions would be reduced lowering the available active sites on Fe-Al-Zr surface [40].

In other words, the adsorption process was hindered in part by excess Na^+ in the solution. Metal ions usually form electric double layer (EDL) complexes with Fe-Al-Zr ternary nanocomposite sorbent. It has been reported [41] that the presence of a cation, such as Na^+, decreases heavy metal ion interaction constants due to the accumulation of charge in the vicinity of the Fe-Al-Zr surfaces. The presence of these cations creates a localized potential that repels other cations, thus reducing the adsorption potentials of the Fe-Al-Zr. Additionally, the ionic strength affected the activity coefficients of Cd (II), Cr (VI) and Pb (II) ions, which limited their transfer to the Fe-Al-Zr ternary nanocomposite sorbent surfaces. Moreover, an increase in ionic strength supplies more positive ions that compete with the heavy metal ions for adsorption sites on the Fe-Al-Zr ternary nanocomposite sorbent so that the adsorption decreased as ion strength increase. It is well known that ions adsorbed by outer-sphere association are strongly sensitive to ionic strength where as ions adsorbed by inner sphere association either show little sensitivity to ionic strength or greater adsorption with increasing ionic strength [30]. Based on this finding, it can be concluded that the metal anions are adsorbed by outer-sphere mechanism as the sorption of all the three ions declined with increase in ionic strength. This result could be corroborated by the absence of any peak related to these metal ions in the XRD analysis done after sorption (Figure 1).

Desorption study

The lead, chromium and cadmium desorbability can be defined as the ratio of the desorbed Cd(II), Cr(VI) and Pb(II) ions over the total adsorbed Cd(II), Cr(VI) and Pb(II) ions by the adsorbent. Therefore, the desorbability can be used to indicate the degree of Cd(II), Cr(VI) and Pb(II) ions desorption from the adsorptive materials. As Figure 7 showed that the desorption of metal ion increases from 9.71 to 32.1% for Cd(II), 16.4-60% for Cr(VI) and from 28.5 to 39.3% for Pb(II) as pH of the solution increases from 2 to 9. These result indicated that desorption was more favorable at higher pH in case of adsorbate ions. Up to pH 6 the desorption of adsorbate ions take place slightly, then after that increased highly. When compared to Pb(II) and Cr(VI) desorption of Cd(II) was more difficult than Pb(II) and Cr(VI) at low pH. For Cd(II), Cr(VI) and Pb(II) ions maximum desorption was obtained at pH 9 (32.1%, 60% and 39.3%) for Cd(II), Cr(VI) and Pb(II), respectively.

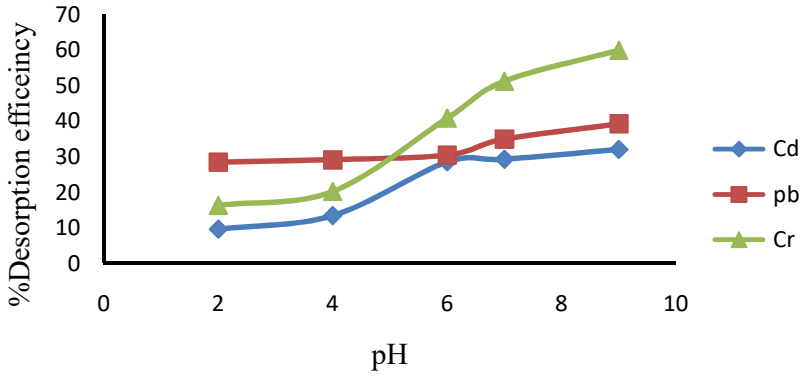

Figure 7. Effect of pH on desorption of Cd(II), Cr(VI) and Pb(II) ions in, nanoparticle mixed oxide of Al-Fe-Zr, respectively at varied pH.

Recycling of Fe-Al-Zr

The recycling and regeneration ability is significant for the practical application of adsorbents. Such adsorbents with excellent adsorption capacity as well as high desorption property will reduce secondary pollution and the overall cost. Thus, the desorption experiments of Fe-Al-Zr were performed to evaluate the recyclability of the sorbent. The used adsorbents were washed by base sodium hydroxide as eluent, and the adsorbed Cd(II), Pb(II) and Cr(VI) ions molecules were efficiently desorbed. It was seen that the adsorption capacity of Cd(II), Pb(II) and Cr(VI) ions adsorbed on as-prepared adsorbent slightly decreased after every cycle of adsorption-desorption process. Therefore, the prepared magnetic nanocomposites are expected to be employed repeatedly and cost-effective in metal ion wastewater treatment.

CONCLUSIONS

In this work, Fe_3O_4-Al_2O_3-ZrO_2 composite was prepared by co-precipitation method. The as-synthesized sorbent was characterized by XRD, SEM-EDX, BET and FTIR techniques. The material appeared amorphous nature with crystalline domains and exhibits relatively better

specific surface area (205 m^2g^{-1}). The removal of Cd(II), Cr(VI) and Pb II) ions by the sorbent was found to be pH dependent, with a maximum retention of Cd(II), Cr(VI) and Pb(II) ions occurred at pH 6, 4 and 6, respectively. Pseudo second-order reaction rate model adequately described the kinetics of sorption of Cd(II), Cr(VI) and Pb(II) ions with high coefficient of determination (R^2 = 0.9958, 0.9998 and 0.9967). Freundlich equations were fitted more for the adsorption process relative to Langmuir. The sorption property of the mixed oxide adsorbent has also been treated with respect to thermodynamic parameters and the sorption process was found to be spontaneous and endothermic. Cd(II), Cr(VI) and Pb(II) ions desorbability was observed to increase with increasing pH indicating that relatively favorable conditions for recycling of the sorbent at higher pH values.

ACKNOWLEDGEMENTS

The authors would like to acknowledge the financial support received from Ministry of Education through the School of Graduate Studies, Haramaya University. The support in characterizing our samples received from Instituto de Catalisis y Petroleoquimica, CSIC, is highly appreciated. The financial support obtained from Haramaya University via project code (HURG-2016-03-02) is also duly acknowledged.

REFERENCES

1. Awokunmi, E.E.; Asaolu, S.S.; Ipinmoroti, K.O. Effect of leaching on heavy metals concentration of soil in some dumpsites. *Sci. Technol.* **2013**, 1, 495–499.
2. Quintelas, C.; Rocha, Z.; Silva, B.; Fonseca, B.; Figueiredo, H.; Tavares, T. Removal of Cd(II), Cr(VI), Fe(III) and Ni(II) from aqueous solutions by an *E . Coli* biofilm supported on kaolin. *Chem. Eng. J.* **2009**, 149, 319–324.
3. Amiri, M.J.; Fadaei, E.; Baghvand, A.; Ezadkhasty, Z. Removal of heavy metals Cr(VI), Cd(II) and Ni(II) from aqueous solution by bioabsorbtion of *Elaeagnus Angustifoli*a. *Int. J. Environ. Res.* **2014**, 8, 411–420.
4. Fetter, C.W. *Contaminant Hydrogeology*, 2nd ed., Upper Saddle River, NJ: Prentice Hall; Prentice-Hall International (UK); London; **1999**; p 387.
5. Tocchi, C.; Federici, E.; Fidati, L.; Manzi, R.; Vincigurerra, V.; Petruccioli, M. Aerobic treatment of dairy wastewater in an industrial three-reactor plant : Effect of aeration regime on performances and on protozoan and bacterial communities. *Water Res.* **2012**, 46, 3334–3344.
6. Wang, L.; Yuan, X.; Zhong, H.; Wang, H.; Wu, Z.; Chen, X.; Zeng, G. Release behavior of heavy metals during treatment of dredged sediment by microwave-assisted hydrogen peroxide oxidation. *Chem. Eng. J.* **2014**, 258, 334–340.
7. Haileyesus, T.; Isabel, D.; Tesfahun, K.; Taddesse, A. M. Synthesis, characterization and photocatalytic activity of zeolite supported $ZnO/Fe_2O_3/MnO_2$ nanocomposites. *J. Environ. Chem. Eng.* **2015**, 3, 1586–1591.
8. Hamad, H.A.; Sadik, W.A.; Abd El-latif, M.M.; Kashyout, A.B.; Feteha, Y.M. Optimizing the preparation parameters of mesoporous nanocrystalline titania and its photocatalytic activity in water: Physical properties and growth mechanisms. *Process Saf. Environ. Prot.* **2015**, 98, 390-398.
9. Ma, X.; Liu, X.; Anderson, D.P.; Chang, P.R. Modification of porous starch for the adsorption of heavy metal ions from aqueous solution. *Food Chem.* **2015**, 181, 133–139.
10. Staj, A.; Onjia, A.; Radovanovi, F. Engineering novel membrane-supported hydrogel for removal of heavy metals. *J. Environ. Chem. Eng.* **2015**, 3, 453–461.
11. Ewecharoen, A.; Thiravetyan, P.; Wendel, E.; Bertagnolli, H. Nickel adsorption by sodium

polyacrylate-grafted activated carbon. *J. Hazard. Mater.* **2009**, 171, 335–339.
12. Karnib, M.; Kabbani, A.; Holail, H.; Olama, Z. Heavy metals removal using activated carbon, silica and silica activated carbon composite. *Energy Procedia* **2014**, 50, 113–120.
13. Pires, C.; Marques, A.P.G.C.; Guerreiro, A.; Magan, N.; Castro, P.M.L. Removal of heavy metals using different polymer matrixes as support for bacterial immobilisation. *J. Hazard. Mater.* **2011**, 191, 277–286.
14. Wang, P.; Du, M.; Zhu, H.; Bao, S.; Yang, T.; Zou, M. Structure regulation of silica nanotubes and their adsorption behaviors for heavy metal ions : pH effect, kinetics, isotherms and mechanism. *J. Hazard. Mater.* **2015**, 286, 533–544.
15. Mohapatra, M.; Anand, S. Synthesis and applications of nano-structured iron oxides/ hydroxides: Review. *Int. J. Eng. Sci. Techn.* **2010**, 2, 127–146.
16. Wakshuma, Y.; Taddesse, A.M.; Kibebew, K.; Nigussie, D. Synthesis and characterization of Fe-Al-Mn nanocomposite sorbent for phosphate sorption-desorption study. *Bull. Chem. Soc. Ethiop.* **2018**, 32, 421–436.
17. Wang, X.; Guo, Y.; Yang, L.; Han, M.; Zhao, J.; Cheng, X. Nanomaterials as Sorbents to Remove Heavy Metal Ions in Wastewater Treatment. *Env. Anal. Toxicol.* **2012**, *2*, 1-7.
18. Reza, A.; Mirrahimi, M.A. Efficient separation of heavy metal cations by anchoring polyacrylic acid on superparamagnetic magnetite nanoparticles through surface modification. *Chem. Eng. J.* **2010**, 159, 264–271.
19. Huang, S.; Chen, D. Rapid removal of heavy metal cations and anions from aqueous solutions by an amino-functionalized magnetic nanoadsorbent. *J. Hazard. Mater.* **2009**, 163, 174–179.
20. Guo, X.; Du, B.; Wei, Q.; Yang, J.; Hu, L.; Yan, L.; Xu, W. Synthesis of amino functionalized magnetic graphenes composite material and its application to remove Cr(VI), Pb(II), Hg(II), Cd(II) and Ni(II) from contaminated water. *J. Hazard. Mater.* **2014**, 278, 211–270
21. Chanani, M.E.; Bahramifar, N.; Younesi, H. Synthesis of Fe_3O_4@silica core – shellparticles and their application for removal of copper ions from water. *J. Appl. Res. Water Wastewater.* **2015**, 2, 176–182.
22. Giraldo, L.; Erto, A.; Moreno-piraja, J.C. Magnetite nanoparticles for removal of heavy metals from aqueous solutions: Synthesis and characterization. *Adsorption* **2013**, 19, 465–474.
23. Fekadu, K.B. *Synthesis and Characterization of $Al_2O_3/Fe_3O_4/ZrO_2$ Heterojunction Ternary Nanocomposite for Nitrate Sorption from Aqueous Solution*. MSc thesis, Haramaya Ehiopia **2015**. http://institutional_repository.haramaya.edu.et/handle/12345 6789
24. Kaewsarn, P.; Saikaew, W.; Wongcharee, S. Dried biosorbent derived from banana peel: A potential biosorbent for removal of cadmium ions from aqueous solution. **201**7, *The 18th Thailand Chemical Engineering and Applied Chemistry Conference October 20-21,2008, Pattaya Thailand No. October 2008. https ://www.researchgate.net/publication/ 317614977.*
25. Gupta, V.K.; Nayak, A. Cadmium removal and recovery from aqueous solutions by novel adsorbents prepared from orange peel and Fe_2O_3 nanoparticles. *Chem. Eng. J.* **2012**, 180, 81–90.
26. Hadjmohammadi, M.R.; Biparva, P.; Sciences, S.A. Removal of Cr(VI) from aqueous solution using pine needles powder as a biosorbent. *J. Appl. Sci. Environ. Sanit*. **2011**,6, 1–13.
27. Khazaei, I.; Branch, B.; Aliabadi, M. Use of agricultural waste for removal of Cr(VI) from aqueous solution use of agricultural waste for removal of Cr(VI) from aqueous solution. *Iran. J. Chem Eng.* **2011**, 8, 11–23
28. Awan, M.; Qazi, I.; Khalid, I. Removal of heavy metals through adsorption using sand. *J. Environ. Sci.* **2003**, 15, 413–416.
29. Ali, R.M.; Hamad, H.A.; Hussein, M.M.; Malash, G.F. Potential of using green adsorbent of

heavy metal removal from aqueous solutions: Adsorption kinetics, isotherm, thermodynamic, mechanism and economic analysis. *Ecol. Eng.* **2016**, 91, 317–332.
30. Abebe, B.; Taddesse, A.M.; Kebede, T.; Teju, E.; Diaz, I. Fe-Al-Mn ternary oxide nanosorbent : Synthesis, characterization and phosphate sorption property. *J. Environ. Chem. Eng.* **2017**, 5, 1330–1340.
31. Mukherjee, R.; De, S. Adsorptive removal of nitrate from aqueous solution by polyacrylonitrile–alumina nanoparticle mixed matrix hollow-fiber membrane. *J. Memb. Sci.* **2014**, 466, 281–292
32. Bandura, L. Sorption of heavy metal ions from aquoues solution by glauconite. *Frensc. Environ. Bull.* **2014**, 23, 825–839.
33. Yohannes, A. *Biosupported Fe-Al-Mn Ternary Oxide Nanosorbent: Synthesis, Characterization and Lead (Pb) Sorption Property in Aqueous Solution*. MSc Thesis, Haramaya University, Haramaya, Ethiopia, **2014**.
34. Semagne, B.; Diaz, I.; Kebede, T.; Taddesse, A.M. Synthesis, characterization and analytical application of polyaniline tin(IV)molybdophosphate composite with nanocrystalline domains. *React Func. Polym.* **2016**, 98, 17–23.
35. Chai, L.; Wang, Y.; Zhao, N.; Yang, W.; You, X. Sulfate-doped Fe_3O_4/Al_2O_3 nanoparticles as a novel adsorbent for fluoride removal from drinking water. *Water Res.* **2013**, 47, 4040–4049.
36. Angel, J.D.; Aguilera, A.F.; Galindo, I.R.; Martínez, M.; Viveros, T. Synthesis and characterization of alumina-zirconia powders obtained by sol-gel method: Effect of solvent and water addition rate. *Mater. Sci. Appl*. **2012**, 3, 650–657.
37. Zare, E.N.; Lakouraj, M.M.; Ramezani, A. Effective adsorption of heavy metal cations by superparamagnetic poly(aniline-co-m-phenylenediamine)@Fe_3O_4 nanocomposite. *Adv. Polym. Technol.* **2015**, 34, 1–11.
38. Yang, G.; Tang, L.; Lei, X.; Zeng, G.; Cai, Y.; Wei, X. Applied surface science Cd(II) removal from aqueous solution by adsorption on α-ketoglutaric acid-modified magnetic chitosan. *Appl. Surf. Sci.* **2014**, 292, 710–716.
39. Zhao, G.; Wu, X.; Tan, X.; Wang, X. Sorption of heavy metal ions from aqueous solutions: A review. *Open Colloid Sci. J.* **2011**, 4, 19–31.
40. Alemu, A.; Lemma, B.; Gabbiye, N.; Tadele, M.; Teferi, M. Removal of chromium(VI) from aqueous solution using vesicular basalt: A potential low cost wastewater treatment system. *Heliyon* **2018**, 4, 1–22.
41. Kosa, S.A.; Al-zhrani, G.; Abdel, M. Removal of heavy metals from aqueous solutions by multi-walled carbon nanotubes modified with 8-hydroxyquinoline. *Chem. Eng. J.* **2012**, 181–182, 159–168.
42. Lu, J.; Liu, H.; Liu, R.; Zhao, X.; Sun, L.; Qu, J. Adsorptive removal of phosphate by a nanostructured Fe-Al-Mn trimetal oxide adsorbent, *Powder Technol*. **2013**, 233, 146–154.
43. Yaswanth, K.P.; Ganapathi, A.; Janakarajan, R.; Kamal, K.K. Redox synergistic Mn-Al-Fe and Cu-Al Fe ternary metal oxide nano adsorbents for arsenic remediation with environmentally stable As(0) formation. *J. Hazard. Mater*. **2019**, 364, 519–530.
44. Hualing, J.; Xueqin, L.; Lei, T.; Tao, W.; Qi, W.; Pingping, N.; Pinghua, C.; Xubiao, L. Defluoridation investigation of yttrium by laminated Y-Zr-Al tri-metal nanocomposite and analysis of the fluoride sorption mechanism. *Sci. Total Environ*. **2019**, 648, 1342–1353.
45. Santos, V.; Zeni, M.; Bergmann, C.P.; Hohemberger, J.M. Correlation between thermal treatment and tetragonal/monochlinic nanostructure zirconia powder obtained by sol-gel process. *Rev. Adv. Mater*. *Sci.* **2008**, 17, 62–70.
46. Felora, H.; Reza B.A. Synthesis and characterization of nanocrystalline zirconia powder by simple sol–gel method with glucose and fructose as organic additives, *Powder Technol.* **2011**, 205, 193–200.